Biology Direct

RESEARCH Open Access

Affibodies as valuable tool to prevent β_2m aggregation under lysosomal-like conditions

Visentin Cristina[1*], Rizzi Giulia[1], Wen Yin[2], Hotot Mathilde[1], Roy Dipambita[1], Gräslund Torbjörn[2], Capelli Riccardo[1] and Ricagno Stefano[1*]

Abstract
Beta-2 microglobulin (β_2m) is a small protein that forms the invariant subunit of the Major Histocompatibility Complex I. Monomeric β_2m is stable under physiological conditions, however high local concentrations can induce misfolding, leading to amyloid deposition. This accumulation has been recently observed in the lysosomes of tumour-associated macrophages from patients affected by multiple myeloma. Such aggregation has been linked to inflammation and tumour progression. Stabilizing the native state of β_2m could be the first step towards preventing this cancer-promoting process. To achieve this goal, the effect of affibody molecules, small and stress-resistant affinity proteins, was tested. Three affibodies molecules were selected against β_2m. Affibody-β_2m complex formation was initially assessed by size exclusion chromatography and subsequently confirmed by microscale thermophoresis and isothermal titration calorimetry. In parallel, in presence of one of the affibody ($Z_{\beta 2m\_01}$) a significant reduction in β_2m aggregation was observed. The inhibition of amyloid formation was also confirmed by transmission electron microscopy. Taken together, these results indicate that $Z_{\beta 2m\_01}$ has the potential to act as β_2m aggregation inhibitor under lysosomal-like pH values.

Keywords Amyloid aggregation, Multiple myeloma, Affibodies, Beta-2 microglobulin, Affinity molecules

Background

Amyloidoses represent a large group of diseases, characterised by the presence of large and insoluble protein deposits in specific tissues [1]. These pathologies can manifest in a localised and organ-specific manner, or systemically, with amyloid deposition spreading to different organs. However, all deposits share common features [2]. It is important to note that all amyloid proteins exist in a physiological soluble form, which, upon misfolding, ultimately results in the formation of toxic insoluble aggregates [2]. These deposits exhibit a distinctive beta-sheets conformation, irrespective of the original protein fold, forming unbranched and elongated fibrils [3]. A further common feature is the reactivity to Congo red and Thioflavin T (ThT).

Beta-2 microglobulin (β_2m) constitutes the light chain of the class I Major Histocompatibility Complex [4] and of the neonatal Fc receptor [5], and is a well-known amyloid protein [6]. Two different scenarios have been identified that trigger β_2m amyloid deposition in humans: (i) high blood concentrations resulting from renal failure and long-term dialysis [7], or (ii) destabilising single point mutations [8–11]. While technological advancements have improved the management of the former condition, the latter remains incurable [6]. Patients affected by

*Correspondence:
Visentin Cristina
cristina.visentin@unimi.it
Ricagno Stefano
stefano.ricagno@unimi.it
[1]Dipartimento di Bioscienze, Università degli Studi di Milano, Milan, Italy
[2]Department of Protein Science, School of Engineering Sciences in Chemistry, Biotechnology and Health, KTH Royal Institute of Technology, Stockholm, Sweden

β_2m-related amyloidoses exhibit amyloid deposits within the extracellular matrix of specific tissues [7, 8, 10, 11], resulting in organ failure or tissue damage. Currently, no treatment options against β_2m aggregation are available for these patients, except for palliative cure. In addition to these primary amyloidoses, a role for β_2m aggregation has been recently reported in the progression of multiple myeloma due to its accumulation within lysosomes, thereby causing lysosome rupture and activating inflammation [12].

Given its pathologic relevance processes, interfering with β_2m aggregation would have far-reaching translational implications. Previous studies have demonstrated that Nb24, a nanobody raised against β_2m, can effectively inhibit the amyloid aggregation of wild type β_2m and of some of its pathological mutants under physiologic conditions [13–15]. Nanobodies have great potential as therapeutic agents against amyloid aggregation [16–18], however in this pathologic context a very high affinity against β_2m is not enough. Indeed in this specific case, the β_2m binder needs a very stable protein scaffold across a range of physiologic conditions and pH values. Affibodies are a class of highly specific binders characterised by a very stable fold.

Thus, in this study, we examined the effect of β_2m-binding affibody molecules in achieving this goal. Affibody molecules are small, non-immunoglobulin-derived affinity proteins, folded in an anti-parallel three-helix bundle conformation [19]. The affibody scaffold is derived from the B-domain of staphylococcal protein A [20], which has a natural affinity for IgG from some species. By randomization of amino acids directly involved in IgG binding and in the vicinity, large combinatorial libraries have been created. Affibody molecules that exhibit strong affinity for desired targets, as distinct from IgG molecules, can be selected from these libraries by means of phage- or cell-display technology [19]. The affibody molecules are characterised by small size (6.5 kDa), resistance to high temperatures, and rapid and reversible folding [21]. They have emerged as one of the most promising alternatives to antibodies. In clinical trials, affibody-based constructs have been found suitable and well tolerated by patients for both therapeutic and diagnostic applications [22, 23]. Thanks to their small size, affibody molecules typically exhibit an efficient extravasation and tissue penetration [24]. Application of affibody molecules in the amyloid research field is limited, despite evidence of their protective action against beta-amyloid aggregation [25–28].

In this study, three distinct affibody molecules were selected to specifically bind β_2m, followed by characterisation and evaluation in relation to their capability to form stable molecular complexes and to impair β_2m aggregation under lysosomal-like conditions, aiming to the identification of an inhibitor against this cancer-promoting process. Selected variants were expressed, purified, and in vitro characterised. Their ability to bind β_2m was assessed by size exclusion chromatography (SEC), and the binding affinity was analysed by microscale thermophoresis (MST) and isothermal titration calorimetry (ITC). The inhibition of β_2m amyloid formation was tested by performing aggregation kinetics monitored by ThT fluorescence and transmission electron microscopy (TEM). Finally, the potential binding site was predicted using AlphaFold3. All these analyses identified one promising affibody variant able to bind β_2m and to impair its aggregation under lysosomal-like pH.

Methods

β_2m expression and purification

β_2m was expressed and purified as reported in [29, 30].

Selection of Affibody molecules

The ectodomain of human FcRn, consisting of the extracellular part of the alpha chain and β_2m, produced in SKOV-3 cells [31], was biotinylated by EZ-Link Sulfo-NHS-LC-Biotin (Thermo Scientific, MA, USA) and used for selection from an affibody library essentially as described [32]. The library had an equal representation of 18 amino acids (cysteine and proline were excluded) in the varied positions [25], and each variant was expressed on phage protein 3 as a fusion to an albumin binding domain (ABD). Target binding was performed in selection buffer (100 mM NaP_i pH 5.5, 150 mM NaCl, 0.1% Tween-20, and 0.1% gelatin) in the absence or presence of 1.5 μM human serum albumin, followed by extensive washing and elution at pH 8.0 (100 mM NaP_i, 150 mM NaCl) or at pH 2.2 (50 mM glycin-HCl). After four rounds of biopanning in the four conditions, eluted phages were used to infect *E. coli* and allowed to form colonies on agar plates. The clones were directly expressed from the colonies in 1 ml cultures in deep well plates at 37 °C. Periplasmic protein expression was induced by the addition of isopropyl-β-D-1-thiogalactopyranoside (IPTG) to a final concentration of 1 mM. The periplasmic fractions were released by freeze-thawing, and the interaction with β_2m was investigated by ELISA. A goat anti-ABD antibody (in-house produced, 2 μg/ml) was immobilized in the wells of a 96-well plate. The periplasmic extracts were then added to capture the affibody-ABD fusion protein of each clone. Biotinylated β_2m (5 μg/ml) was added to wells followed by Horseradish peroxidase-conjugated Streptavidin (1:30000 dilution) and TMB substrate (Thermo Scientific) according to the manufacturer's protocol.

Affibody expression and purification

The DNA sequences of three affibody variants: $Z_{\beta 2m\_01}$, $Z_{\beta 2m\_02}$, and $Z_{\beta 2m\_03}$, and a control Z_{Taq}, were optimised

for expression in *E. coli* and purchased by GENEWIZ GmbH (Germany) as synthetic genes cloned into a pET28c expression vector between *EcoRI* and *NdeI* restriction sites. The recombinant proteins carry a C-terminal 6XHis-tag and a thrombin recognition site. $Z_{\beta 2m\_01}$ was expressed in the Shuffle *E. coli* strain. Briefly, transformed cells were grown at 30 °C in Luria Bertani (LB) medium supplemented with 25 μg/mL kanamycin until an OD_{600} of 0.8 was reached. Protein expression was then induced by the addition of 1 mM IPTG for 20 h at 16 °C. The protein expression of $Z_{\beta 2m\_02}$, $Z_{\beta 2m\_03}$ and Z_{Taq} was performed in BL21(DE3) pLysS *E. coli* strain. Briefly, transformed cells were grown at 37 °C in LB medium supplemented with 25 μg/mL kanamycin until OD_{600} 0.8 was reached. The induction of protein expression was achieved by adding 1mM IPTG for 4 h at 37 °C. The purification of all four affibody molecules was performed using the same protocol. The cell pellet was resuspended in 20 mM Tris HCl, 150 mM NaCl, 20 mM imidazole, 1 mM phenylmethanesulfonyl fluoride, pH 8.0 supplemented with 0.1 mg/ml DNase I and complete Protease inhibitor cocktail. Post-sonication, the crude extract was subjected to a 30 min centrifugation at 30,900 *rcf* at 4 °C. Thereafter, the supernatant was filtered using 0.45 μm syringe filters, and subsequently subjected to HIS-trap affinity chromatography (HisTrap™ Fast Flow, Cytiva). The column was equilibrated in 20 mM Tris-HCl, 150 mM NaCl, 20 mM Imidazole, pH 8.0 and the proteins were eluted in a gradient 0-100% of 20 mM Tris-HCl, 150 mM NaCl, 500 mM Imidazole, pH 8.0. The fractions containing the protein were collected and subjected to a size exclusion chromatography using a SuperdexTM 75 Increase 10/300 GL (Cytiva) previously equilibrated in 20 mM Tris-HCl, 150 mM NaCl, pH 7.4.

Circular dichroism assay

β_2m or the affibody molecules were diluted at 0.2 mg/ml in 20 mM buffer (Sodium phosphate for pH 7.4, 7.0, 6.5, 6.0; Sodium acetate for pH 5.5, 5.0. 4.5, 4.0, 3.5, 3.0, 3.5, 2.0). Far-UV spectra were collected on a J-1500 spectrophotometer (Jasco) equipped with a Peltier system for temperature control recording the signal at 25 °C between 195 nm and 260 nm wavelength range in a 0.1 cm path length quartz cuvette. The mean residual ellipticity ($[\theta]_{MRW,\lambda}$) [33] is reported. Temperature ramps were recorded from 25 °C to 80 °C at a heating rate of 1 °C/min while monitoring the circular dichroism (CD) signal at 202 nm. T_m values were determined as the maximum of the first derivative of the unfolding profiles. Every experiment was repeated in duplicate.

Analytical size exclusion chromatography

A solution of 50 μM β_2m and 100 μM affibody molecule, with a molar ratio 1: 2, was prepared in 20 mM NaP_i, 150 mM NaCl, pH 7.4 and subsequently analysed using a ProteoSEC SEC column (CliniSciences) previously equilibrated in the same buffer. Every experiment was repeated in triplicate.

Microscale thermophoresis

MST analyses were performed at 25 °C on a NanoTemper NT.115 instrument. The affibody molecules were diluted in PBS-T buffer (20 mM NaH_2PO_4/Na_2HPO_4 pH 7.4, 20 mM NaCl, 0.05% Tween) and labelled with RED-tris-NTA 2nd Generation dye (Nanotemper) in accordance with the manufacturer's protocol. β_2m was freshly prepared before each experiment by dissolving lyophilised aliquots in PBS-T buffer. The binding between β_2m and the affibody molecules was monitored by titrating β_2m into 25 nM labelled affibody, using the red filter, 40% LED power and medium MST power. Prior to measurement, samples were incubated for 30 min in the dark and then loaded into NanoTemper Premium capillaries. Every experiment was repeated in triplicate. Data analysis was carried out using NanoTemper Analysis software using the K_D model fitting (one binding site) and plotted using Prism9.

Isothermal titration calorimetry

β_2m and $Z_{\beta 2m\_01}$ or $Z_{\beta 2m\_03}$ were buffer exchanged to 20 mM Tris-HCl, 150 mM NaCl, pH 7.4. ITC measurements were performed using a microcal PEAQ ITC calorimeter (Malvern). The cell temperature was set to 37 °C and the syringe stirring speed to 750 rpm. β_2m was loaded into the cell at a concentration of 40 μM, whereas the affibody molecules were loaded into the syringe at concentrations ranging from 400 to 600 μM. Affibody to buffer titrations were performed as controls. Shown data were only baseline-corrected, since dilution effects upon titration were not evident. Every experiment was repeated in triplicate. Data and binding parameters were assessed using the MicroCal Peak ITC software (Malvern) and analyzed using a two-state binding model by fixing the stoichiometry of the binding at 1.

Aggregation assay

β_2m was diluted to 200 μM (2.4 mg/ml) in the presence or absence of 400 μM affibody in 20 mM Sodium Acetate, pH 4.5 or 20 mM Tris-HCl, pH 7.4. Freshly prepared Thioflavin T (ThT) was added to a final concentration of 20 μM. As control, a solution of 400 μM affibody was also analysed. 50 μL of each condition was then pipetted into black polystyrene 96-well half-area plates with clear bottoms and polyethylene glycol coating (Corning). Each condition was performed in triplicate in each experiment. Plates were sealed to prevent evaporation and incubated at 37 °C under mild agitation in a Varioskan Lux plate reader (Thermo Fisher Scientific). Upon excitation at

450 nm, fluorescence at 480 nm was recorded through the bottom of the plate with the interval between measurements set at 10 min for a total duration of 150 h. Each experiment was performed at least in triplicate. The mean ThT fluorescence values from the independent experiments were plotted using Prism9 and subjected to nonlinear regression analysis using a sigmoidal equation.

Transmission electron microscopy

At the end of the aggregation assay, 10 µl of the mixture containing only β_2m or β_2m and $Z_{\beta 2m\_01}$ were analysed by TEM. A 10 µl droplet of sample was applied onto a 400-mesh copper carbon-coated grid (Agar Scientific). After 1 min incubation, excess of sample was removed and the grid was stained with 2% (w/v) uranyl acetate solution, blotted dry, and imaged on a Talos L120C transmission electron microscope (Thermo Fisher Scientific) operating at 120 kV.

AlphaFold structure predictions

To model the four complexes, between the affibody molecules and β_2m, the AlphaFold3 algorithm [34] was employed. Operatively, the sequence of $Z_{\beta 2m\_01}$ and $Z_{\beta 2m\_02}$ were used as input, performing 20 runs of the algorithm with different initialization seeds (from 1 to 20). For every run, five structures were generated, selecting for each complex the top 20 among all the predictions, following the AlphaFold3 reliability score, defined as

$$0.8 \times ipTM + 0.2 \times pTM + 0.5 \times disorder - 100 \times has\_clash$$

Where:

- *-ipTM* is the confidence score of the multimer interface (ranging from 0 to 1);
- *-pTM* is the confidence score of the monomer prediction (ranging from 0 to 1);
- *-disorder* is the fraction of the residues in the input which is classified as disordered.
- *-has_clash* is a boolean indicating if the structure has a significant number of clashing atoms (more of 50% or more than 100).

Results

β_2m behaviour at lysosomal-like pH

β_2m is a well-studied protein and its biophysical properties and aggregation propensity at physiologic [35] or very acidic pH (pH 2.5) have been reported [36, 37]. However, a detailed molecular characterisation of β_2m at intermediate acidic pH corresponding to lysosomal pH (pH 4–5) is still lacking. For this reason, we first determined its fold stability at decreasing pH values (Fig. 1A-B). β_2m was resuspended under different pH conditions and CD spectra were acquired to evaluate the secondary structure content. As shown in Fig. 1A, β_2m fully retains its native fold down to pH 5.0, while it is completely lost at pH 3.5 and below. The signal at 202 nm was then analysed to derive an apparent pH_m (Fig. 1B), defined as pH value at which half of the protein molecules in solution are unfolded, which was calculated to be 4.7. The thermal stability was also investigated by increasing the temperature of a solution of β_2m at both pH 7.4 and pH 4.5. The results in Fig. 1C show that at acidic pH, the derived apparent T_m, the inflection point of the unfolding curve, is lowered by almost 20 °C compared to physiological pH (62.1 °C at pH 7.4 vs. 44.5 °C at pH 4.5). Finally, β_2m aggregation kinetics at pH 7.4 or pH 4.5 were evaluated incubating the protein at 37 °C under shaking. As shown in Fig. 1D, a significant ThT fluorescence increase, indicating protein aggregation, was observed only at a lysosome-like pH value.

Affibody selection

To generate affibody molecules, a large combinatorial library of affibody molecules displayed on phage were subjected to selections as previously described [32]. After four rounds of selection, 192 clones were analysed by ELISA to identify β_2m-binders. This screening yielded several variants interacting with β_2m from all four selection tracks, and the three with the highest ELISA signal, $Z_{\beta 2m\_01}$, $Z_{\beta 2m\_02}$, and $Z_{\beta 2m\_03}$, were selected for further analyses. Z_{Taq} was used as a negative control, being developed to bind to DNA polymerase from *Thermus aquaticus*.

Affibody expression and characterisation

The affibody molecules were expressed as His-tagged proteins and purified from the soluble fraction through HisTrap affinity chromatography followed by a SEC. Their secondary structure content was analysed by CD spectroscopy, which showed structures with high alpha-helical content (Fig. 2). Affibody molecules are often stable and resilient to extreme environments, and we therefore determined their fold stability at different pH values. As shown in Fig. 2, all three β_2m-binding variants and the control show a high alpha-helical content even at extremely low pH values (pH 2.0).

$Z_{\beta 2m\_01}$ and $Z_{\beta 2m\_02}$ are able to form complexes with β_2m. The binding affinity of the affibody molecules and β_2m was explored using different approaches. First, a mixture of β_2m in the presence of a 2-fold molar excess of the affibody molecule was prepared and analysed by SEC. In the presence of $Z_{\beta 2m\_01}$ or $Z_{\beta 2m\_02}$, the elution profile of the solution containing both affibody molecules and β_2m, exhibited two peaks, corresponding to the affibody-β_2m complexes and to free affibody, respectively (Fig. 3A

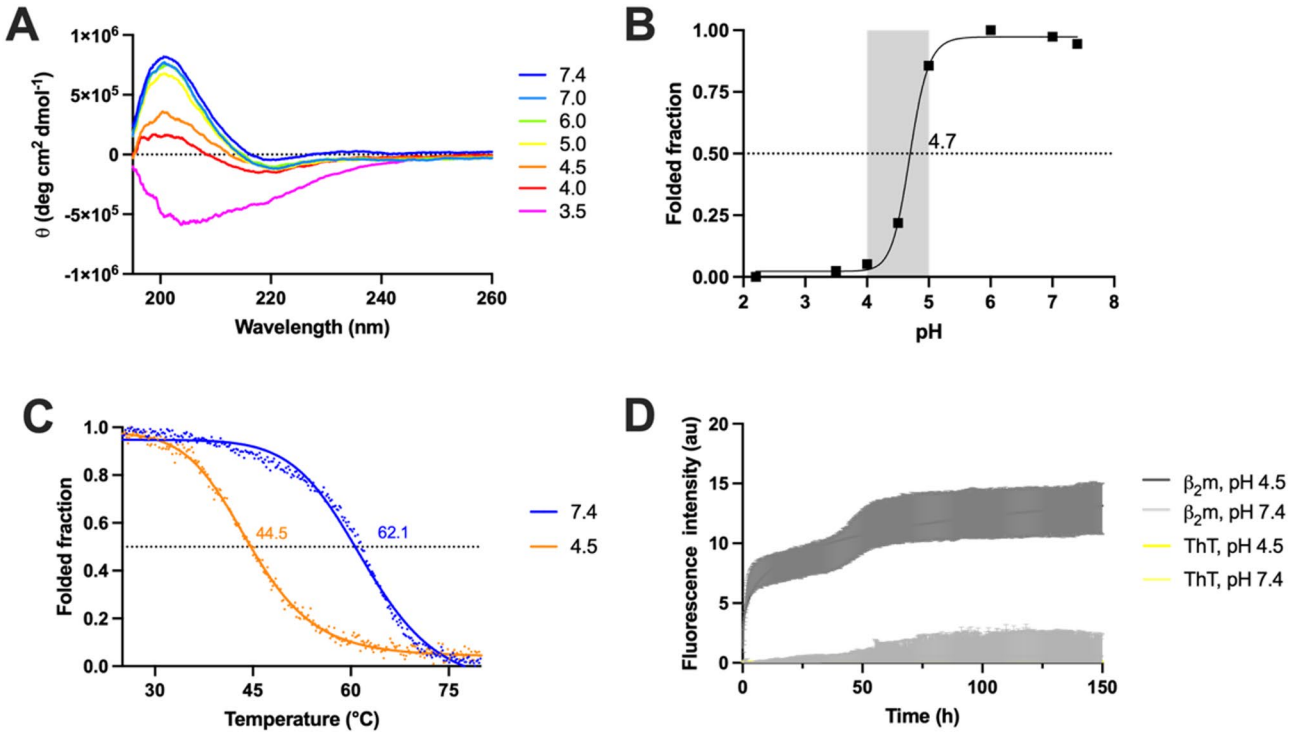

Fig. 1 β_2m stability. (**A**) The Far-UV spectra of 0.2 mg/ml β_2m at different pH values were collected at 25 °C monitoring the CD signal between 195 and 260 nm. Data are reported as molar ellipticity. (**B**) pH-dependent denaturation curve in the 2.5–7.4 pH range was derived plotting the CD signal at 202 nm collected at different pH values and normalised as folded fraction. The grey area highlights the range of lysosomal pH. (**C**) Thermal denaturation at pH 7.4 and 4.5 was performed monitoring the CD signal at 202 nm while increasing the temperature from 25 to 80 °C with a 1 °C/min rate. Data are expressed as folded fraction. (**D**) Aggregation kinetics of 200 μM β_2m at pH 7.4 or 4.5 at 37 °C under agitation while monitoring ThT fluorescence. As a control 20 μM ThT (same concentration used in the presence of β_2m) was incubated under identical conditions.

and B). In the presence of the control Z_{Taq} (Fig. 3D) and $Z_{\beta 2m\_03}$ (Fig. 3C), no clear shifts in peak elution were observed, ruling out the formation of affibody-β_2m complexes. For comparison, isolated affibody molecules and β_2m were also analysed by SEC, obtaining single peaks.

To corroborate the SEC observations and derive equilibrium dissociation constants (K_D values) for the affibody-β_2m interactions, MST analyses were carried out (Fig. 4A and S1). The MST experiments could only detect the interaction between $Z_{\beta 2m\_01}$ and β_2m, yielding a K_D of 189±40 nM (Fig. 4A). For Z_{Taq}, $Z_{\beta 2m\_02}$ and $Z_{\beta 2m\_03}$ instead no binding was observed (Fig S1).

Then, ITC analyses were performed to further characterise the binding between the affibody molecules and β_2m (Fig. 4B and C). These analyses confirmed the complex formation between $Z_{\beta 2m\_01}$ and β_2m, with a derived K_D in the nanomolar range (12.9±5.6 nM). The ΔH between bound and unbound is -6.8±0.4 kcal/mol, and the molar ratio of interaction has been calculated as 1:1. Interestingly, ITC could monitor the formation of the $Z_{\beta 2m\_02}$-β_2m complex although characterised by a rather weak interaction (K_D 33.1±12.5 μM). The ΔH between bound and unbound is -3.2±0.2 kcal/mol, and the molar ratio of interaction was calculated as 1:1.

$Z_{\beta 2m\_01}$ inhibits β_2m aggregation at lysosomal-like conditions

Thus, to test the capability of the affibody molecules to inhibit β_2m aggregation under lysosomal-like conditions, aggregation assays were performed at pH 4.5 at a protein concentration well in line with the β_2m concentration observed in multiple myeloma patients (2.4 mg/ml in the test *vs* 2.5 mg/ml in patients) [38]. β_2m was diluted in the presence or absence of a 2-fold molar excess of affibody and incubated at 37 °C for 150 h, while amyloid aggregation was monitored by registering the ThT fluorescence signal over the time (Fig. 5A and B and S2). As a control, the aggregation of the affibody molecules alone or β_2m was also tested under the same conditions. Isolated β_2m aggregated efficiently at pH 4.5, reaching a plateau after 24 h. Isolated affibody molecules displayed different aggregation propensities: $Z_{\beta 2m\_01}$ and Z_{Taq} remained soluble over the time and no increased ThT signal was observed, conversely, $Z_{\beta 2m\_02}$ and $Z_{\beta 2m\_03}$ exhibited a rapid increase in ThT signal indicating their aggregation under the tested conditions (Fig. 5A and S2). Intriguingly, while β_2m aggregated undisturbed in the presence of Z_{Taq}, $Z_{\beta 2m\_01}$ demonstrated to be able to prevent β_2m aggregation. Unexpectedly the aggregation kinetics

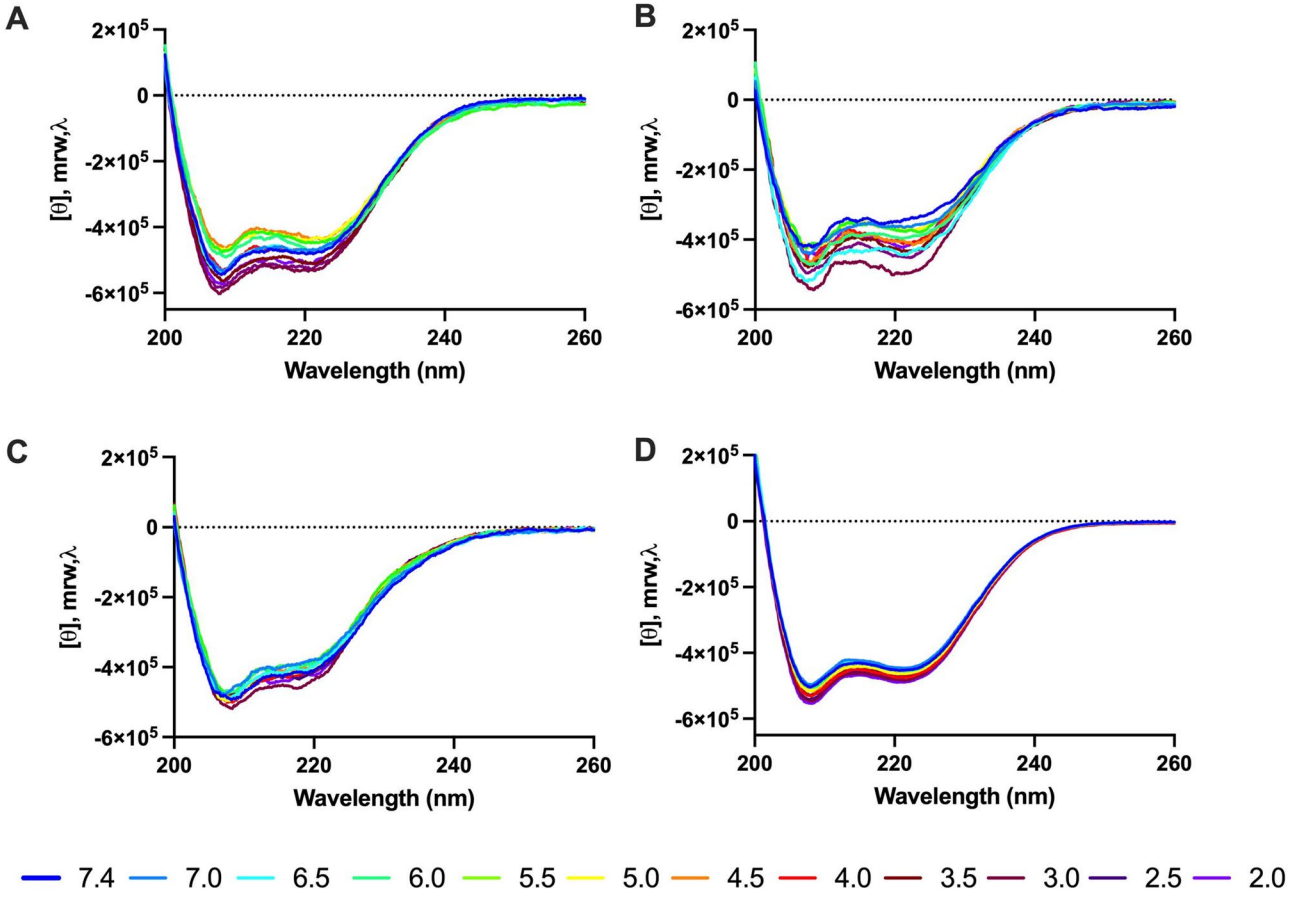

Fig. 2 Affibodies chemical stability. The Far-UV spectra of 0.2 mg/ml solution of $Z_{\beta 2m\_01}$ (**A**), $Z_{\beta 2m\_02}$ (**B**), $Z_{\beta 2m\_03}$ (**C**), and Z_{Taq} (**D**) were collected at 25 °C monitoring the CD signal between 200 and 260 nm at different pH values. Data are reported as molar ellipticity.

at acidic pH showed a biphasic trend. Since at such pH native and unfolded β_2m seem to coexist, the denatured β_2m molecules may aggregate more promptly than the native or native like molecules accounting for the aggregation profile observed in Figs. 1D and 5A. To better highlight the impact of the different affibody molecules on β_2m aggregation, the mean ThT fluorescence at the plateau of the aggregation process is reported in Fig. 5B. This figure further points out the fold stability of native $Z_{\beta 2m\_01}$ under lysosomal-like pH and its ability to prevent β_2m aggregation.

Finally, samples of β_2m alone and in the presence of $Z_{\beta 2m\_01}$ were analysed by TEM. As shown in Fig. 5C and D, β_2m alone formed the characteristic amyloid aggregates, whereas in the presence of $Z_{\beta 2m\_01}$ no fibrillar aggregates were observed.

Structural models of affibody- β_2m complexes

To identify the mode of interaction between $Z_{\beta 2m\_01}$ or $Z_{\beta 2m\_02}$ and β_2m, a series of structure predictions to model the affibody-β_2m complexes were performed using AlphaFold3 [34]. Considering the distribution of the 20 best predictions, the average pLDDT score, *i.e.*, a metric that evaluates the confidence of the predicted fold, was similar for both $Z_{\beta 2m\_01}$-β_2m and $Z_{\beta 2m\_02}$-β_2m complexes around 75/100 (a score greater than 70 is considered reliable) (Fig. 6B). However, considering the scores distribution, it seemed that the algorithm was only able to accurately model the $Z_{\beta 2m\_01}$-β_2m complex, while for the $Z_{\beta 2m\_02}$-β_2m complex the evaluation of the folding obtained resulted less conclusive, in agreement with experimental data. Indeed, considering the confidence in the interface (iPTM score– Fig. 6C), the variance observed in the pLDDT was present also in the iPTM, which measures the accuracy of the predicted relative positions of the subunits forming the protein-protein complex, for $Z_{\beta 2m\_02}$ (Fig. 6A).

The complex interface between $Z_{\beta 2m\_01}$ and $Z_{\beta 2m\_02}$ with β_2m was analysed. $Z_{\beta 2m\_01}$ and $Z_{\beta 2m\_02}$ interact with β_2m using almost the same residues, which are located in the known affibody-interaction region (Fig. S3). Instead, Fig. 6D lists β_2m residues predicted to be involved in binding: even though not identical $Z_{\beta 2m\_01}$ and $Z_{\beta 2m\_02}$ are predicted to bind the same β_2m region thus they assemble in very similar quaternary structures. In particular, the residues of β_2m involved in affibody binding are

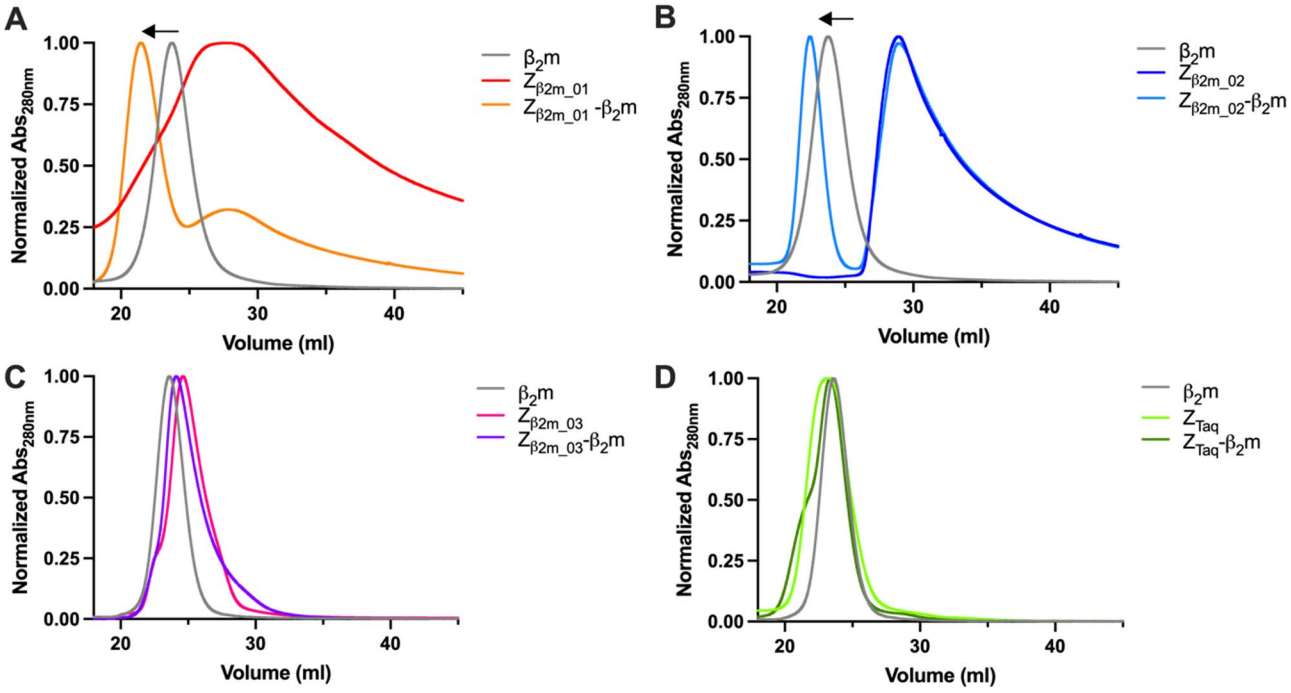

Fig. 3 SEC analysis of affibody and β_2m complex formation. A solution of β_2m was incubated in the absence or presence of 2-fold molar excess of affibody molecules. The ability of $Z_{\beta2m\_01}$ (**A**), $Z_{\beta2m\_02}$ (**B**), $Z_{\beta2m\_03}$ (**C**) and Z_{Taq} (**D**) to form a complex with β_2m was evaluated by SEC. As control, solutions of affibody molecules and of β_2m alone diluted at the same concentrations were analysed by SEC. The absorbance at 280 nm is reported as normalized data.

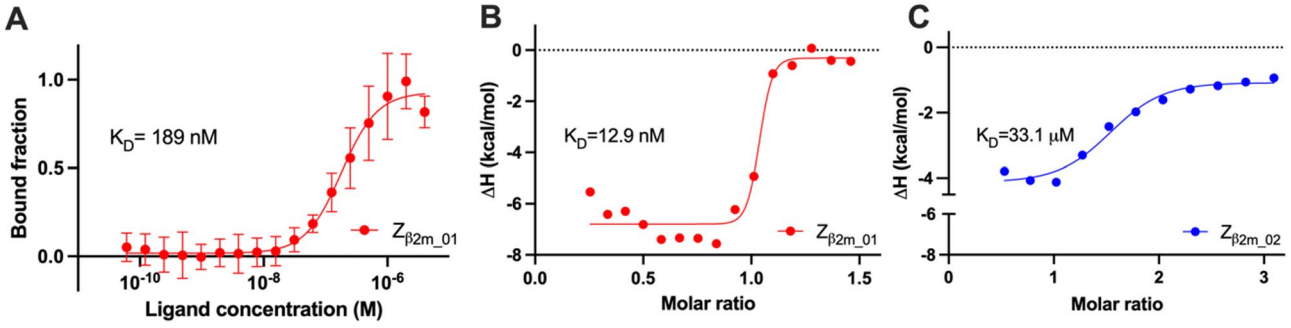

Fig. 4 Determination of $Z_{\beta2m\_01}$ and $Z_{\beta2m\_02}$ binding affinity for β_2m. (**A**) Determination of the affinity of $Z_{\beta2m\_01}$ to β_2m by MST. $Z_{\beta2m\_01}$ was labelled with RED-tris-NTA 2nd Generation dye, and β_2m was titrated using a concentration range between 4 μM and 0 nM. (**B**-**C**) The binding affinity was measured by ITC at 37 °C titrating $Z_{\beta2m\_01}$ (**B**) or $Z_{\beta2m\_02}$ (**C**) into 20 μM β_2m. The resulting data were analysed using Prism9. MTS and ITC data have been fitted using a sigmoidal function or a Boltzmann sigmoidal function, respectively.

located in strand A, the end of strand B and a larger area corresponding to strand D, loopDE, strand E. $Z_{\beta2m\_01}$ seemed to have a slightly less extended area of interaction (pink and red residues) compared to $Z_{\beta2m\_02}$ (pink and blue residues).

Discussion

It is well established that the process of β_2m aggregation in dialysis-related amyloidosis is linked to elevated levels of β_2m in the blood [39] and this process has been extensively studied [6]. Abnormally high levels of β_2m have also been identified in multiple myeloma patients (up to 2.5 mg/ml) [38], although its full role in multiple myeloma pathogenesis remains to be explored. Hofbauer et al. reported in 2021 that elevated β_2m levels result in aggregation inside tumour-associated macrophages, thereby sustaining inflammation and facilitating abnormal B-cell proliferation [12]. This is attributed to the elevated local concentration of β_2m within the lysosomes of tumour-associated macrophages, in concurrence with the local acidic pH and the presence of proteases. The consequence of this scenario is amyloid aggregation, leading to the swelling of lysosomes and their subsequent rupture [12]. It is well known that very low pH facilitates β_2m aggregation [29, 40], but no detailed biophysical characterisation was available at lysosomal-like

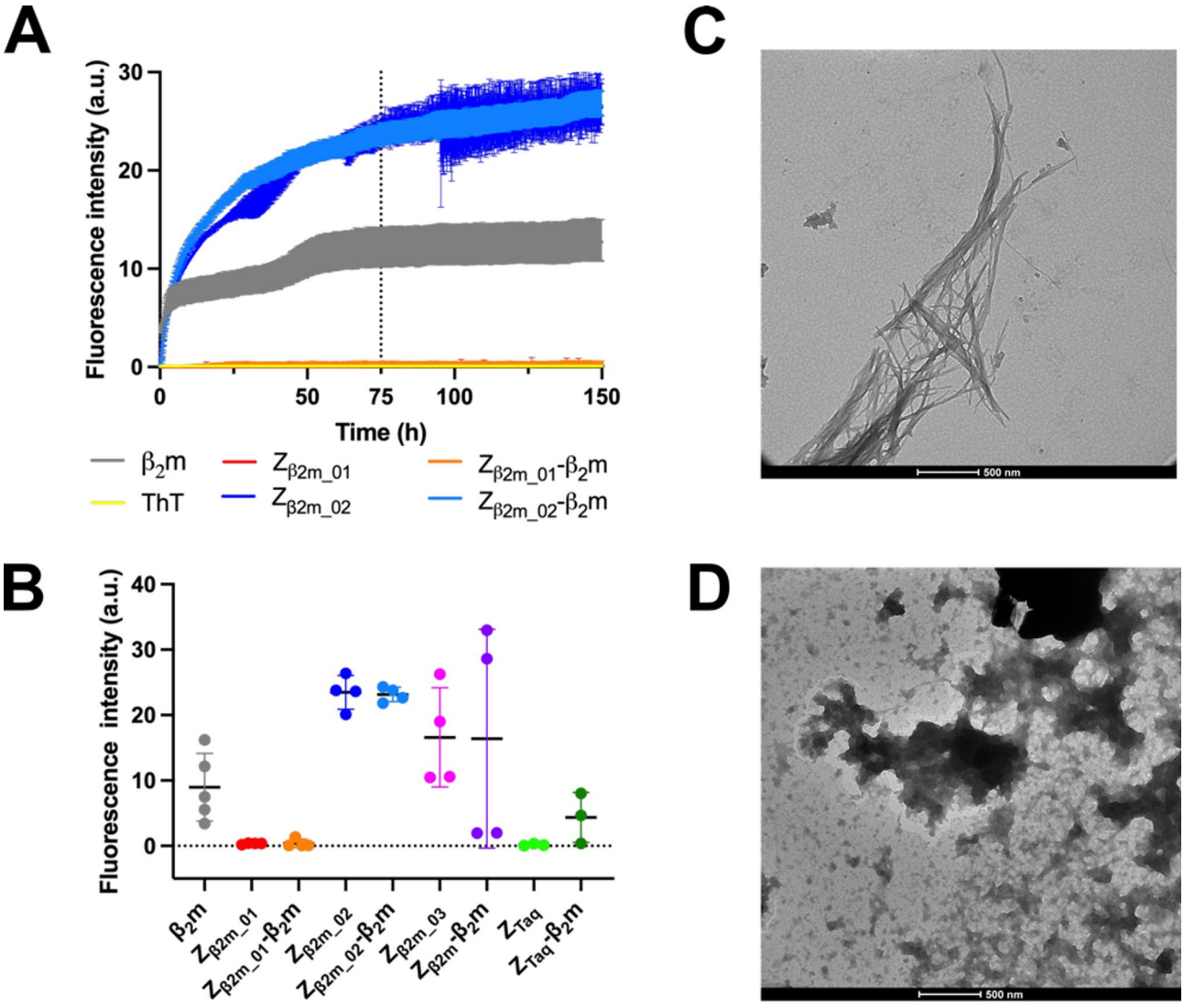

Fig. 5 Aggregation under lysosomal-like conditions. (**A**) Aggregation kinetics of 200 μM β_2m alone or in the presence of $Z_{\beta2m\_01}$ or $Z_{\beta2m\_03}$ at a 1:2 molar ratio were monitored following ThT fluorescence over 150 h at 37 °C under agitation. Data were fitted using a sigmoidal function. (**B**) ThT fluorescence values after 75 h of incubation. Data are reported as mean values and standard deviation. (**C-D**) TEM analyses of β_2m alone (**C**) or in the presence of $Z_{\beta2m\_01}$ (**D**) at the end of the aggregation assay.

pH (4.0–5.0). Therefore, we evaluated the impact of pH 4.5, an intermediate value in the lysosomal pH range, on β_2m molecular properties. Both chemical and thermal stability assessments revealed that at pH 4.5, β_2m is still broadly in its native conformation, though highly destabilised, leading to accelerated and extensive aggregation (Fig. 1). These observations provide substantial evidence to support the hypothesis that aggregation is facilitated under the conditions present in lysosomal lumen as recently proposed by Hofbauer et al. [12].

The aim of this study was to generate affibody molecules capable of inhibiting β_2m m aggregation. Such binders should ideally be resistant to unfolding at acidic pH, so that the complex with β_2m would be stable in the lysosomal lumen of tumour-associated macrophages. We chose to use affibodies for this purpose since they are robust molecules, resistant to chemical and thermal stress [41].

A set of affibody molecules specifically binding to β_2m was generated. These proteins were then expressed, purified, and their chemical stability was assessed. Crucially, all affibody molecules displayed a native, highly alpha-helical, structure at acidic pH (Fig. 2). SEC analyses revealed that $Z_{\beta2m\_01}$ and $Z_{\beta2m\_02}$ were able to complex with β_2m (Fig. 3).

Subsequently, MST and ITC analyses were performed (Fig. 4, S1) to assess the complex affinity. Both MST and ITC provided K_D-values in the nanomolar range for the $Z_{\beta2m\_01}$-β_2m complex (Fig. 4). On the contrary, only ITC detected the formation of the low-affinity

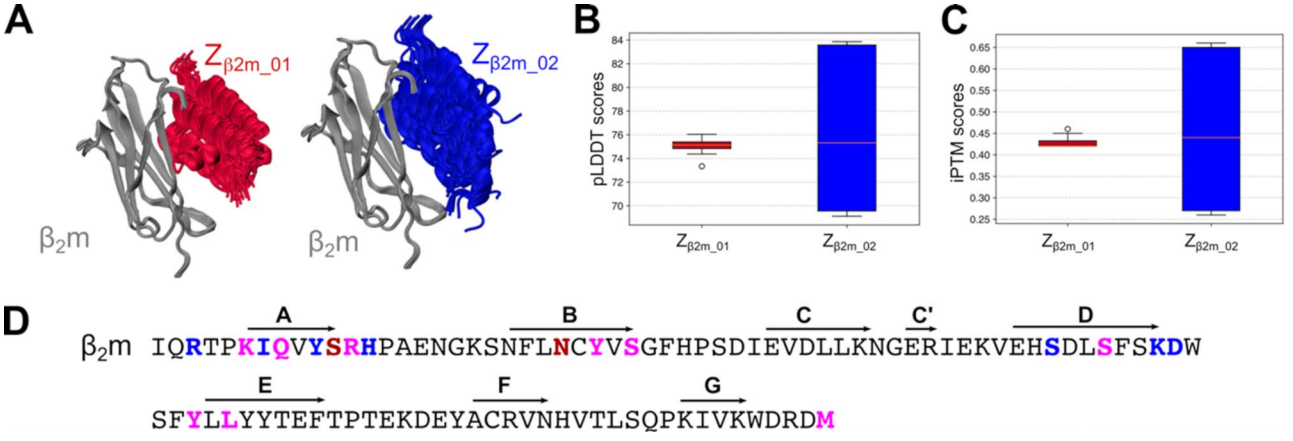

Fig. 6 Comparison of AlphaFold3 predictions for affibody-$β_2$m complexes. (**A-B**) Cartoon representations of $β_2$m in complex with $Z_{β2m\_01}$ (left), and $Z_{β2m\_02}$ (right). (**B**) pLDDT score distribution for the complexes $Z_{β2m\_01}$-$β_2$m and $Z_{β2m\_02}$-$β_2$m. (**C**) iPTM score distribution for the complexes $Z_{β2m\_01}$-$β_2$m and $Z_{β2m\_02}$-$β_2$m. (**D**) $β_2$m residues involved in the interaction with $Z_{β2m\_01}$ (red), $Z_{β2m\_02}$ (blue) or both affibody molecules (pink).

complex between $Z_{β2m\_02}$ and $β_2$m (Fig. 4 and S1). This discrepancy may be partially attributed to the labelling of the affibody molecules necessary for MST analysis. As expected from these analyses, no binding was observed with Z_{Taq} or $Z_{β2m\_03}$. Binding studies were performed at physiological pH representing the pH value present in the extracellular space where the affibody-$β_2$m interaction may take place.

Subsequently, we tested the affibody molecules as inhibitors of $β_2$m aggregation under lysosomal pH. The aggregation assay was therefore performed at pH 4.5, and ThT fluorescence was monitored over time. Consistently, $Z_{β2m\_01}$ was the only tested affibody able to completely abolish $β_2$m aggregation as shown in Fig. 5. Moreover, a significant increase in ThT signal was detected in isolated $Z_{β2m\_02}$ and $Z_{β2m\_03}$ samples preventing a solid evaluation of their efficacy as β2m aggregation inhibitors (Fig. 5A and B and S2). The nature of such ThT positive species was not studied in detail, given that $Z_{β2m\_02}$ and $Z_{β2m\_03}$ display poor binding and no binding to β2m, respectively.

The ability of $Z_{β2m\_01}$ to prevent $β_2$m aggregation was also investigated by TEM analysis (Fig. 5C and D), showing that the presence of $Z_{β2m\_01}$ completely abolished the formation of amyloid aggregates, which were instead abundant in samples of isolated $β_2$m. Indeed, the elongated assemblies typical of amyloid fibrils visible in Fig. 5C are absent in Fig. 5D. Thus, both ThT-monitored aggregation kinetics and TEM analysis point at a putative protective effect of $Z_{β2m\_01}$ against $β_2$m aggregation.

To rationalize the experimental observations, we simulated the capability of $Z_{β2m\_01}$ and $Z_{β2m\_02}$ to bind $β_2$m using AlphaFold3 software (Fig. 6). The software consistently predicted the formation of a complex with an average pLDDT score > 75 (Fig. 6B), even though the pLDDT score for $Z_{β2m\_02}$ presented high variability. This suggests that the fold identification was unstable. This hypothesis was corroborated by the analysis of the iPTM values, which are indicative of the confidence for the predicted interface. Thus, in keeping with experimental data, AlphaFold3 prediction indicates that $Z_{β2m\_01}$ is forming a stable complex with a reliable fold prediction (pLDDT = 75) and consistent evaluation of the interface (iPTM ~ 0.43) suggesting qualitative information on the complex assembly.

The predicted $β_2$m region interacting with $Z_{β2m\_01}$ covered strand A, the end of strand B and a large area spanning to strand D, DE loop, and strand E. The ability of $Z_{β2m\_01}$ to prevent $β_2$m aggregation can be rationalised by assuming that $Z_{β2m\_01}$ interaction stabilises such $β_2$m regions which are known hotspots that determine $β_2$m aggregation propensity. The unstable ΔN6-$β_2$m truncated variant (lacking the first 6 amino acids) directly demonstrates the stabilising role of strand A for the native $β_2$m fold [42]. Ample published evidence points to strand D and loop DE as critical determinants of fold stability and aggregation propensity [43–46]. $Z_{β2m\_02}$ is also predicted to interact with the same $β_2$m region, however its apparent inability to counteract $β_2$m aggregation may be explained by a very low binding affinity for $β_2$m.

In conclusion, we identified $Z_{β2m\_01}$, an affibody molecule that demonstrated the capability to form a stable complex with $β_2$m, thereby preventing its aggregation under lysosomal-like conditions. This finding has thus identified a novel molecule with the potential to block the $β_2$m-driven production of pro-inflammatory signals aggravating and sustaining multiple myeloma resilience and progression.

Abbreviations

$β_2$m	Beta-2 microglobulin
CD	Circular dichroism
ITC	Isothermal titration calorimetry
MST	Microscale thermophoresis

SEC Size exclusion chromatography
TEM Transmission electron microscopy

Supplementary Information

The online version contains supplementary material available at https://doi.org/10.1186/s13062-025-00659-2.

Supplementary Material 1

Acknowledgements
Unitech NOLIMITS at Università degli Studi di Milano for the TEM analyses.

Author contributions
SR, TG, and CV designed the work; CV, HM, RD, WY, TG, GR, and RC acquired, analysed, and interpretated the data; CV, SR, RC, and TG have drafted the work, all the authors revised the manuscript.

Funding
Fondazione AIRC per la ricerca sul cancro ETS IG 2024 ID 30307 to SR. The Swedish Cancer Society (Cancerfonden): 21 1861 Pj 01 H and 24 3883 Pj 01 H. Knut och Alice Wallenbergs Stiftelse (KAW). Fondazione U. Veronesi is gratefully acknowledged for the support to CV.

Data availability
All the raw AlphaFold3 prediction data and the best model obtained are available on a public repository hosted by Zenodo (https://doi.org/10.5281/zenodo.15120889).

Declarations

Competing interests
The authors declare no competing interests.

Clinical trial number
Not applicable.

Received: 11 April 2025 / Accepted: 26 May 2025
Published online: 06 June 2025

References

1. Buxbaum JN, Eisenberg DS, Fändrich M, McPhail ED, Merlini G, Saraiva MJM, Sekijima Y, Westermark P. Amyloid nomenclature 2024: update, novel proteins, and recommendations by the international society of amyloidosis (ISA) nomenclature committee. Amyloid. 2024;31:249–56. https://doi.org/10.1080/13506129.2024.2405948.
2. Merlini G, Bellotti V. Molecular mechanisms of amyloidosis. N Engl J Med. 2003;349:583–96. https://doi.org/10.1056/NEJMra023144.
3. Chiti F, Dobson CM. Protein misfolding, functional amyloid, and human disease. Annu Rev Biochem. 2006;75:333–66. https://doi.org/10.1146/annurev.biochem.75.101304.123901.
4. Ploegh HL, Orr HT, Strominger JL. Major histocompatibility antigens: the human (HLA-A,-B,-C) and murine (H-2K, H-2D) class I molecules. Cell. 1981;24:287–99. https://doi.org/10.1016/0092-8674(81)90318-4.
5. Simister NE, Creighton J, Ahouse. The structure and evolution of FcRn. Res Immunol. 1996;147:333–7. https://doi.org/10.1016/0923-2494(96)89647-7.
6. Portales-Castillo I, Yee J, Tanaka H, Fenves AZ. Beta-2 microglobulin amyloidosis: past, present, and future, Kidney360 1 (2020) 1447–55. https://doi.org/10.34067/KID.0004922020
7. Gejyo F, Yamada T, Odani S, Nakagawa Y, Arakawa M, Kunitomo T, Kataoka H, Suzuki M, Hirasawa Y, Shirahama T. A new form of amyloid protein associated with chronic Hemodialysis was identified as beta 2-microglobulin. Biochem Biophys Res Commun. 1985;129:701–6. https://doi.org/10.1016/0006-291x(85)91948-5.
8. Valleix S, Gillmore JD, Bridoux F, Mangione PP, Dogan A, Nedelec B, Boimard M, Touchard G, Goujon J-M, Lacombe C, Lozeron P, Adams D, Lacroix C, Maisonobe T, Planté-Bordeneuve V, Vrana JA, Theis JD, Giorgetti S, Porcari R, Ricagno S, Bolognesi M, Stoppini M, Delpech M, Pepys MB, Hawkins PN, Bellotti V. Hereditary systemic amyloidosis due to Asp76Asn variant β2-microglobulin. N Engl J Med. 2012;366:2276–83. https://doi.org/10.1056/NEJMoa1201356.
9. Mizuno H, Hoshino J, So M, Kogure Y, Fujii T, Ubara Y, Takaichi K, Nakaniwa T, Tanaka H, Kurisu G, Kametani F, Nakagawa M, Yoshinaga T, Sekijima Y, Higuchi K, Goto Y, Yazaki M. Dialysis-related amyloidosis associated with a novel β2-microglobulin variant. Amyloid. 2021;28:42–9. https://doi.org/10.1080/13506129.2020.1813097.
10. Prokaeva T, Joshi T, Klimtchuk ES, Gibson VM, Spencer B, Siddiqi O, Nedelkov D, Hu Y, Berk JL, Cuddy SAM, Dasari S, Chiu A, Choate LA, McPhail ED, Cui H, Chen H, Burks EJ, Sanchorawala V, Connors LH. A novel substitution of proline (P32L) destabilises β2-microglobulin inducing hereditary systemic amyloidosis. Amyloid. 2022;29:255–62. https://doi.org/10.1080/13506129.2022.2072199.
11. Haslett JJ, Patel JK, Kittleson MM. Beta 2-microglobulin: case report of a rare cause of cardiac amyloidosis. Eur Heart J Case Rep. 2023;7:ytad239. https://doi.org/10.1093/ehjcr/ytad239.
12. Hofbauer D, Mougiakakos D, Broggini L, Zaiss M, Büttner-Herold M, Bach C, Spriewald B, Neumann F, Bisht S, Nolting J, Zeiser R, Hamarsheh S, Eberhardt M, Vera J, Visentin C, De Luca CMG, Moda F, Haskamp S, Flamann C, Böttcher M, Bitterer K, Völkl S, Mackensen A, Ricagno S, Bruns H. β2-microglobulin triggers NLRP3 inflammasome activation in tumor-associated macrophages to promote multiple myeloma progression. Immunity. 2021;54:1772–e17879. https://doi.org/10.1016/j.immuni.2021.07.002.
13. Domanska K, Vanderhaegen S, Srinivasan V, Pardon E, Dupeux F, Marquez JA, Giorgetti S, Stoppini M, Wyns L, Bellotti V, Steyaert J. Atomic structure of a nanobody-trapped domain-swapped dimer of an amyloidogenic beta2-microglobulin variant. Proc Natl Acad Sci U S A. 2011;108:1314–9. https://doi.org/10.1073/pnas.1008560108.
14. Vanderhaegen S, Fislage M, Domanska K, Versées W, Pardon E, Bellotti V, Steyaert J. Structure of an early native-like intermediate of β2-microglobulin amyloidogenesis. Protein Sci. 2013;22:1349–57. https://doi.org/10.1002/pro.2321.
15. Raimondi S, Porcari R, Mangione PP, Verona G, Marcoux J, Giorgetti S, Taylor GW, Ellmerich S, Ballico M, Zanini S, Pardon E, Al-Shawi R, Simons JP, Corazza A, Fogolari F, Leri M, Stefani M, Bucciantini M, Gillmore JD, Hawkins PN, Valli M, Stoppini M, Robinson CV, Steyaert J, Esposito G, Bellotti V. A specific nanobody prevents amyloidogenesis of D76N β2-microglobulin in vitro and modifies its tissue distribution in vivo. Sci Rep. 2017;7:46711. https://doi.org/10.1038/srep46711.
16. Kasturirangan S, Li L, Emadi S, Boddapati S, Schulz P, Sierks MR. Nanobody specific for oligomeric beta-amyloid stabilizes nontoxic form. Neurobiol Aging. 2012;33:1320–8. https://doi.org/10.1016/j.neurobiolaging.2010.09.020.
17. Broggini L, Barzago MM, Speranzini V, Schulte T, Sonzini F, Giono M, Romeo M, Milani P, Caminito S, Mazzini G, Rognoni P, Merlini G, Pappone C, Anastasia L, Nuvolone M, Palladini G, Diomede L, Ricagno S. Nanobodies counteract the toxicity of an amyloidogenic light chain by stabilizing a partially open dimeric conformation. J Mol Biol. 2023;435:168320. https://doi.org/10.1016/j.jmb.2023.168320.
18. Haynes JR, Whitmore CA, Behof WJ, Landman CA, Ong HH, Feld AP, Suero IC, Greer CB, Gore JC, Wijesinghe P, Matsubara JA, Wadzinski BE, Spiller BW, Pham W. Targeting soluble amyloid-beta oligomers with a novel nanobody. Sci Rep. 2024;14:16086. https://doi.org/10.1038/s41598-024-66970-6.
19. Ståhl S, Gräslund T, Eriksson A, Karlström FY, Frejd P-Å, Nygren J, Löfblom. Affibody molecules in biotechnological and medical applications. Trends Biotechnol. 2017;35:691–712. https://doi.org/10.1016/j.tibtech.2017.04.007.
20. Nord K, Gunneriusson E, Ringdahl J, Ståhl S, Uhlén M, Nygren PA. Binding proteins selected from combinatorial libraries of an alpha-helical bacterial receptor domain. Nat Biotechnol. 1997;15:772–7. https://doi.org/10.1038/nbt0897-772.
21. Feldwisch J, Tolmachev V. Engineering of affibody molecules for therapy and diagnostics. Methods Mol Biol. 2012;899:103–26. https://doi.org/10.1007/978-1-61779-921-1_7.
22. Alhuseinalkhudhur A, Lubberink M, Lindman H, Tolmachev V, Frejd FY, Feldwisch J, Velikyan I, Sörensen J. Kinetic analysis of HER2-binding ABY-025 affibody molecule using dynamic PET in patients with metastatic breast cancer. EJNMMI Res. 2020;10:21. https://doi.org/10.1186/s13550-020-0603-9.
23. Gerdes S, Staubach P, Dirschka T, Wetzel D, Weirich O, Niesmann J, da Mota R, Rothhaar A, Ardabili M, Vlasitz G, Feldwisch J, Osterling Koskinen L, Ohlman S, Peloso PM, Brun NC, Frejd FY. Izokibep for the treatment of moderate-to-severe plaque psoriasis: a phase II, randomized, placebo-controlled,

double-blind, dose-finding multicentre study including long-term treatment. Br J Dermatol. 2023;189:381–91. https://doi.org/10.1093/bjd/ljad186.
24. Schmidt MM, Wittrup KD. A modeling analysis of the effects of molecular size and binding affinity on tumor targeting. Mol Cancer Ther. 2009;8:2861–71. https://doi.org/10.1158/1535-7163.MCT-09-0195.
25. Grönwall C, Jonsson A, Lindström S, Gunneriusson E, Ståhl S, Herne N. Selection and characterization of affibody ligands binding to alzheimer amyloid B peptides. J Biotechnol. 2007;128:162–83. https://doi.org/10.1016/j.jbiotec.2006.09.013.
26. Lindberg H, Härd T, Löfblom J, Ståhl S. A truncated and dimeric format of an affibody library on bacteria enables FACS-mediated isolation of amyloid-beta aggregation inhibitors with subnanomolar affinity. Biotechnol J. 2015;10:1707–18. https://doi.org/10.1002/biot.201500131.
27. Wahlberg E, Rahman MM, Lindberg H, Gunneriusson E, Schmuck B, Lendel C, Sandgren M, Löfblom J, Ståhl S, Härd T. Identification of proteins that specifically recognize and bind protofibrillar aggregates of amyloid-β. Sci Rep. 2017;7:5949. https://doi.org/10.1038/s41598-017-06377-8.
28. Salahuddin P, Khan RH, Furkan M, Uversky VN, Islam Z, Fatima MT. Mechanisms of amyloid proteins aggregation and their Inhibition by antibodies, small molecule inhibitors, nano-particles and nano-bodies. Int J Biol Macromol. 2021;186:580–90. https://doi.org/10.1016/j.ijbiomac.2021.07.056.
29. Esposito G, Ricagno S, Corazza A, Rennella E, Gümral D, Mimmi MC, Betto E, Pucillo CEM, Fogolari F, Viglino P, Raimondi S, Giorgetti S, Bolognesi B, Merlini G, Stoppini M, Bolognesi M, Bellotti V. The controlling roles of Trp60 and Trp95 in beta2-microglobulin function, folding and amyloid aggregation properties. J Mol Biol. 2008;378:887–97. https://doi.org/10.1016/j.jmb.2008.03.002.
30. Ramon A, Ali M, Atkinson M, Saturnino A, Didi K, Visentin C, Ricagno S, Xu X, Greenig M, Sormanni P. Assessing antibody and nanobody nativeness for hit selection and humanization with abnativ. Nat Mach Intell. 2024;6:74–91. https://doi.org/10.1038/s42256-023-00778-3.
31. Seijsing J, Lindborg M, Löfblom J, Uhlén M, Gräslund T. Robust expression of the human neonatal Fc receptor in a truncated soluble form and as a full-length membrane-bound protein in fusion with eGFP. PLoS ONE. 2013;8:e81350. https://doi.org/10.1371/journal.pone.0081350.
32. Seijsing J, Lindborg M, Höidén-Guthenberg I, Bönisch H, Guneriusson E, Frejd FY, Abrahmsén L, Ekblad C, Löfblom J, Uhlén M, Gräslund T. An engineered affibody molecule with pH-dependent binding to FcRn mediates extended circulatory half-life of a fusion protein. Proc Natl Acad Sci U S A. 2014;111:17110–5. https://doi.org/10.1073/pnas.1417717111.
33. Kelly SM, Jess TJ, Price NC. How to study proteins by circular dichroism. Biochim Biophys Acta. 2005;1751:119–39. https://doi.org/10.1016/j.bbapap.2005.06.005.
34. Abramson J, Adler J, Dunger J, Evans R, Green T, Pritzel A, Ronneberger O, Willmore L, Ballard AJ, Bambrick J, Bodenstein SW, Evans DA, Hung C-C, O'Neill M, Reiman D, Tunyasuvunakool K, Wu Z, Žemgulytė A, Arvaniti E, Beattie C, Bertolli O, Bridgland A, Cherepanov A, Congreve M, Cowen-Rivers AI, Cowie A, Figurnov M, Fuchs FB, Gladman H, Jain R, Khan YA, Low CMR, Perlin K, Potapenko A, Savy P, Singh S, Stecula A, Thillaisundaram A, Tong C, Yakneen S, Zhong ED, Zielinski M, Žídek A, Bapst V, Kohli P, Jaderberg M, Hassabis D, Jumper JM. Accurate structure prediction of biomolecular interactions with alphafold 3. Nature. 2024;630:493–500. https://doi.org/10.1038/s41586-024-07487-w.
35. Stoppini M, Bellotti V. Lessons from β2-Microglobulin*. J Biol Chem. 2015;290:9951–8. https://doi.org/10.1074/jbc.R115.639799.
36. Iadanza MG, Silvers R, Boardman J, Smith HI, Karamanos TK, Debelouchina GT, Su Y, Griffin RG, Ranson NA, Radford SE. The structure of a β2-microglobulin fibril suggests a molecular basis for its amyloid polymorphism. Nat Commun. 2018;9:4517. https://doi.org/10.1038/s41467-018-06761-6.
37. McParland VJ, Kalverda AP, Homans SW, Radford SE. Structural properties of an amyloid precursor of beta(2)-microglobulin. Nat Struct Biol. 2002;9:326–31. https://doi.org/10.1038/nsb791.
38. Rossi D, Fangazio M, De Paoli L, Puma A, Riccomagno P, Pinto V, Zigrossi P, Ramponi A, Monga G, Gaidano G. Beta-2-microglobulin is an independent predictor of progression in asymptomatic multiple myeloma. Cancer. 2010;116:2188–200. https://doi.org/10.1002/cncr.24959.
39. Scarpioni R, Ricardi M, Albertazzi V, De Amicis S, Rastelli F, Zerbini L. Dialysis-related amyloidosis: challenges and solutions. Int J Nephrol Renovasc Dis. 2016;9:319–28. https://doi.org/10.2147/IJNRD.S84784.
40. Debelouchina GT, Platt GW, Bayro MJ, Radford SE, Griffin RG. Intermolecular alignment in β2-Microglobulin amyloid fibrils. J Am Chem Soc. 2010;132:17077–9. https://doi.org/10.1021/ja107987f.
41. Hosse RJ, Rothe A, Power BE. A new generation of protein display scaffolds for molecular recognition. Protein Sci. 2006;15:14–27. https://doi.org/10.1110/ps.051817606.
42. Esposito G, Michelutti R, Verdone G, Viglino P, ÁNdez HH, Robinson CV, Amoresano A, Piaz FD, Monti M, Pucci P, Mangione P, Stoppini M, Merlini G, Ferri G, Bellotti V. Removal of the N-terminal hexapeptide from human β2-microglobulin facilitates protein aggregation and fibril formation. Protein Sci. 2000;9:831–45. https://doi.org/10.1110/ps.9.5.831.
43. Ricagno S, Raimondi S, Giorgetti S, Bellotti V, Bolognesi M. Human beta-2 microglobulin W60V mutant structure: implications for stability and amyloid aggregation. Biochem Biophys Res Commun. 2009;380:543–7. https://doi.org/10.1016/j.bbrc.2009.01.116.
44. Azinas S, Colombo M, Barbiroli A, Santambrogio C, Giorgetti S, Raimondi S, Bonomi F, Grandori R, Bellotti V, Ricagno S, Bolognesi M. D-strand perturbation and amyloid propensity in beta-2 microglobulin. FEBS J. 2011;278:2349–58. https://doi.org/10.1111/j.1742-4658.2011.08157.x.
45. Ami D, Ricagno S, Bolognesi M, Bellotti V, Doglia SM, Natalello A. Structure, stability, and aggregation of β-2 microglobulin Mutants: insights from a fourier transform infrared study in solution and in the crystalline state. Biophys J. 2012;102:1676–84. https://doi.org/10.1016/j.bpj.2012.02.045.
46. Camilloni C, Sala BM, Sormanni P, Porcari R, Corazza A, De Rosa M, Zanini S, Barbiroli A, Esposito G, Bolognesi M, Bellotti V, Vendruscolo M, Ricagno S. Rational design of mutations that change the aggregation rate of a protein while maintaining its native structure and stability. Sci Rep. 2016;6:25559. https://doi.org/10.1038/srep25559.

Publisher's note